Combining acoustic tracking and hydrodynamic modelling to study migratory behaviour of Atlantic salmon (Salmo Salar) smolts on entry into high-energy coastal waters

McIlvenny, Jason; Williamson, Benjamin; Goddijn-Murphy, Lonneke; Del Villar-Guerra, Diego; Gauld, Niall R

Published in:
ICES Journal of Marine Science

Publication date:
2021

Combining acoustic tracking and hydrodynamic modelling to study migratory behaviour of Atlantic salmon (*Salmo salar*) smolts on entry into high-energy coastal waters

Mcilvenny, J[1]., Youngson, A[1]., Williamson, B.J.[1]., Gauld, N. R[2]., Goddijn- Murphy, L[1] &. Del Villar-Guerra, D[3]

1. Environmental Research Institute, University of the Highlands and Islands, Thurso, Scotland
2. Marine Scotland Science, Scotland
3. Loughs Agency, Northern Ireland

Abstract

Migration from fresh water to the marine environment is a crucial, transitional stage in the development of Atlantic salmon (*Salmo salar*). This study used a combination of acoustic tracking, instrument data and hydrodynamic modelling to examine behaviour of juvenile salmon (smolts) during their transition from fresh water to the marine environment. The study focuses on a high-energy coastal environment in northern Scotland, which is currently being developed for renewable energy extraction and where there is potential for negative impacts on salmon with energy extraction devices and structures. Thirty-four smolts were captured in the River Wick in Caithness and tagged with acoustic tags transmitting at 69 kHz. The Telemac-Mascaret modelling suite was utilised to construct a 3-dimensional model of the study area and surrounding waters to estimate smolt-current interactions during detection times. Timing of migration was linked to low-light conditions, with smolts mainly exiting the river at night and when the moon was below the horizon. The movement of most of the tags conformed with modelled tidal currents and the tracks matched modelled marine tidal patterns. Smolts were detected only on a single tide suggesting that they rapidly cleared the vicinity of the receiver array.

1. Introduction

There is a lack of information regarding the behaviour of out-migrating juvenile Atlantic salmon (*Salmo salar*), known as smolts, and their use of coastal waters (McCormack et al. 1998; Moriarty et al, 2016; Strøm et al. 2018, Ounsley et al. 2020). This knowledge gap is particularly important because these coastal waters are high-energy environments that are increasingly being developed for generation of marine renewable energy via tidal-flow, wind and wave devices. Numerous productive rivers of high conservation value that also support high-value salmon fisheries discharge into the same coastal waters (Malcolm et al. 2010). There is therefore potential for negative interactions between renewable developments and migrating smolts (Malcolm et al. 2010). Potential impacts are physical impact, acoustic and electromagnetic impacts (Bartlett & Thompson 2012). The extent of this risk is unknown because the full migratory behaviour of the fish is unknown in relation to planned or existing renewable energy developments.

In the northern rivers, juvenile salmon spend one or two years in fresh water before entering the smolt stage in early summer when they migrate to the marine environment (Buck & Youngson, 1982; Malcolm et al. 2015). Mortality rates among smolts are reportedly high (Alerstam et al. 2003; Halfyard et al. 2012; Chaput et al. 2018; Lothian et al. 2017, Newton et al. 2016) indicating that migration is a critical stage of the life cycle (Thorstad et al., 2012). Currently, Atlantic salmon are in decline throughout their range for various reasons such as global warming, fisheries impacts and changes in freshwater habitats (Lothian et al. 2017; Nicola et al. 2018) and better understanding of the fishes' behaviour at the critical smolt stage of development may aid improved management.

After entering the marine environment, smolts ultimately migrate to feeding grounds in the distant North Atlantic (Holst et al 2000; Haugland et al 2006; Dadswell et al. 2010; Lefèvre et al. 2012). However, the behavioural mechanisms that support smolt migration between their

initial entry to the marine environment and their subsequent appearance on the ocean feeding grounds are largely undocumented. Moreover, given the Atlantic salmon's wide range and the disparate characteristics of the various coastal waters that local groups of smolts must traverse, varying forms of behaviour must be invoked. There is a lack of information on smolt movement into and through high-energy coastal waters.

To examine potential interactions between renewable energy devices and salmon, contact location and contact duration must be identified. Hydrodynamic modelling offers a means of addressing these questions. This study gathers empirical data of tracks of tagged smolts in a tidally energetic coastal environment and compares observed results with outputs of a 3-dimensional hydrodynamic model to investigate, firstly, if a hydrodynamic model with free drifting particles can simulate tag detection results; secondly, to investigate if smolt are utilising the currents; and thirdly, to investigate the intrinsic directionality of smolt movement. The hypothesis is that the ultimate destination of smolts leaving the Wick river lies far to the west and north of the British mainland (Freidland, 1998; Holst et al. 2000). It is likely therefore that successful completion of the smolt migration is dependent on an intrinsic northwards vector to swimming activity. Additional objectives are to determine the timing of river exit and entry to the marine environment (day/night), and smolt swim depth once in the marine environment.

2. Methods

2.2 Study area

The study was conducted on the Wick River in Northern Scotland (Figure 1). The lower reaches of the river have a straight channel with few gentle meanders and a low gradient prior to the river entering Wick Bay, which is delineated by headlands, North Head and South Head, ca.

1.8 km distance from the river's junction with the bay. (Figure 1). A line of marine detection stations was placed at the seaward limit of the bay (Figure 1).

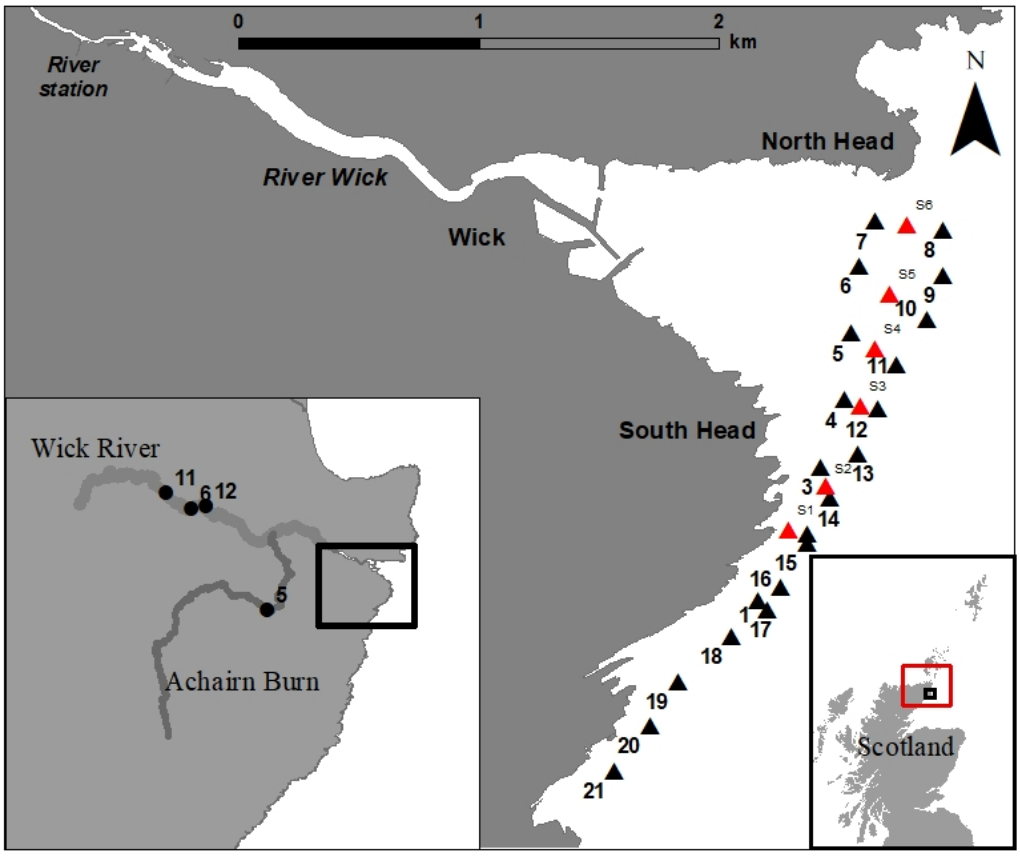

Figure 1: Wick River in North East Scotland: Red rectangle in in-set indicates hydrodynamic model extent. The position of river and marine detection stations are shown (black triangles in large scale map). Sentinel tag locations are shown by red triangles. Circular markers in the lower-left inset show fish capture locations with number caught. Black rectangles are extent indicators of higher scale maps.

2.3 Acoustic tracking

The tracking system comprised Automatic Listening Stations (ALS, Innovasea, Canada; Model VR2) and a mixture of acoustic ID (ID-LP7) and ID-depth (ADT-LP7) transmitter tags (Thelma Biotel, Norway). The ID-LP7 tags transmitted unique codes at 69 kHz and were programmed to transmit at random intervals of between 20 and 40 seconds. The ADT-LP7 depth tags transmitted at fixed intervals of 29, 31 and 33 seconds to avoid crosstalk. The battery life of the tags was estimated at approximately 90 days (manufacturer estimate). A single ALS (River Station, Figure 1) was positioned in a linear section of Wick River of uniform channel dimensions just above the limit of saline influence at 58.4487° N, 3.1227° W (Figure 1). The

River ALS had unobstructed acoustic reception over the approximately 200-m linear river reach. The River ALS was positioned in mid-water where the river was ca. 0.6 m in depth during the study period and the channel ca. 15 m wide.

Twenty-one marine ALS were deployed at spacings of ca. 200 m in a double array design with micro-siting spanning the outer edge of Wick Bay (Figure 1). Previous studies have shown a 200-400 m detection range limit for these sensors (Clements et al 2011; Singh et al. 2010, Hedger et al. 2008), therefore the lowest range was assumed for deployment to provide overlap between adjacent ALS. The receivers were buoyed at 2 m above the seabed using a moored configuration of a bottom weight, line and flotation buoy attached above. The array was biased towards the south side of the bay with the aim of optimising fish detection based on a preliminary assessment of the tidal dynamics in Wick bay. All the ALS were in place before fish tagging commenced. Six ID-LP7 sentinel tags were permanently positioned within part of the marine ALS array in order to continuously monitor the operational characteristics of in-range ALS over the natural range of sea and tidal conditions. The sentinel tags were buoyed to 1 m above the seabed. The ALS signal detections were downloaded on logger recovery. Innovasea loggers process acoustic signals internally and VUE-software (Innovasea) was used to download and quality control detections before logging in a database. Further post-processing quality control proved necessary and this was carried out as detailed below. A Wald–Wolfowitz runs test was performed on the frequency of detections for the marine ALS stations to test whether the smolt frequency detection differed significantly from random. A binomial generalised linear model (GLM) was used to model probability of detection from the sentinel tag dataset. Explanatory variables were distance from receiver, date and current magnitude and direction, with current data derived from the hydrodynamic modelling data. Site range testing confirmed detection ranges of >80% probability of detection at 200 m from

sentinel tag data. 200-meter spacing ensured a large overlap between the detection limits of adjacent stations.

2.4 Fish capture

On 23-24 April 2016, 34 smolts were captured by electro fishing over several locations (Figure 1) in the Wick River catchment. After capture, fish were placed in an aerated holding tank until they were tagged. Large smolts of greater than 130 mm in length were selected for tagging. Fish were anaesthetised using a 0.4 g l-1 solution of MS222 (Tricaine Pharmaq, Pharmaq Ltd, Fordingbridge, Hampshire, United Kingdom) until the fish no longer responded to external stimuli. The smolts were measured and weighed before being placed on a v-shaped surgical board with the ventral body surface facing upward. An incision approximately 13 mm in length was made just off the ventral midline, anterior to the pelvic girdle. The acoustic tag (ID-LP7.3 or ADT-LP7.3, Thelma Biotel, Trondheim, Norway) was inserted through the incision into the body cavity and the incision was closed with two interrupted absorbable vicryl sutures (Ethicon, Johnson and Johnson, Maidenhead, UK, 4-0 suture with a reverse cutting needle). The fish were retained in an in-river recovery box for 1 hr and released at the point of capture. By this point they had fully regained consciousness and responded to external stimuli. All fish were tagged under UK Home Office license by trained personnel.

2.5 Hydrodynamic modelling

A hydrodynamic model was used to predict astronomical tidal conditions during the times of tag detections, comprising flow speed, direction and tide height. The TELEMAC-MASCARET suite was used (Galland et al., 1991), comprising an integrated suite of solvers for use in the

field of free-surface flow. A 3-dimensional model was constructed of Wick Bay and surrounding influential waters including the Pentland Firth area (Figure 1). Telemac-3D was utilised with the non-hydrostatic version of the code and the K-E turbulence closure model in both vertical and horizontal directions. Bathymetric data were extracted from the 1 Arcsecond Bathymetry - Marine Themes Digital Elevation Model available from Edina Digimap (© British Crown and OceanWise, 2018. All rights reserved. Licence No. EK001-20180802). The hydrodynamic model was calibrated using the friction coefficient to tidal data available from the Wick tidal gauge (British Oceanographic Data Centre), and bottom-mounted ADCP data collected in the Pentland Firth by the Environmental Research Institute. A Chezy coefficient value of 44 (corresponding to a roughness Cd value of 0.005; Mcilvenny et al. 2020) was found to have the best fit to the data. This agrees with previous suggested values for the Pentland Firth area (Easton et al., 2012; Rahman & Venugopal, 2015). The model was run using an unstructured grid with a spatial resolution of 10 m around the area of Wick Bay. Elsewhere the grid resolution varied from 2 km in open ocean to 200 m near coast and 500 m near open water boundaries. 5 vertical depth layers were used in the grid (supplementary material, Figure 2).

Free-floating particles were simulated using the Blue-Kenue Software (Canadian Hydraulics centre) and its in-built 'Psed' Lagrangian sediment transport model. Free floating particles were simulated by creating particles with a neutral buoyancy. Particle models were mobilised using the current data from the TELEMAC-MASCARET model. Previous research has found particle modelling of smolts to be a useful indicator of their behaviour at sea (Mork et al. 2012; Byron et al. 2014; Newton et al. 2017).

Several assumptions are necessary to model the movement of a tag based on detections. As the precise location of the first tag detection within a receiver's detection limit is unknown, the starting position for free floating particle insertion must be estimated. In addition, the detection range of each receiver is unknown. This value may be dependent on site-specific conditions at

the time of the detection including current low speed, turbulence, and ambient noise from e.g., sediment movement. A detection range of 200 m was used for each listening station based on the range detection testing done on site prior to fish tagging. For each initial detection time, several locations were tested as the free-drifting particle release point. Particles were released in lines of 500 free-drifting particles with neutral buoyancy at the surface layer orientated across current, to 5 m depth. Several release points were used to determine if currents alone could be responsible for the tag detections patterns observed after initial detection. Hydrodynamic model data were extracted for each tag detection time. Where free particle paths interacted with the tag detection ALS stations within the time frame of tag detections the particle was deemed to have explained the tag detections, thereby model flow only can explain the tag detections. A single free particle was selected from those which explained the tag movement and the particle path length, time and ground speed were calculated. When a tag's timing of detections did not correspond to free drift in tidal current flow indicated by the modelling results, hypothetical movements through the zones of detection were tested. Tidal currents were then averaged over each zone to estimate the maximum and minimum current conditions the tag may have encountered at the surface, the mid-depth and the bed-depth (Figure 2).

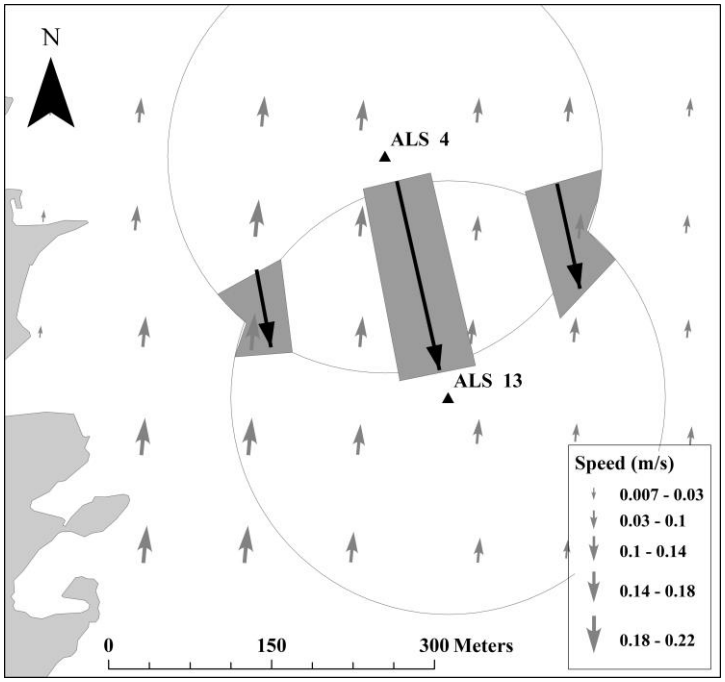

Figure 2: Example: Tag 102 was first detected in ALS 4 and then in ALS 13, against the flow of tidal current at the time (grey arrows). Zones (grey patches) around hypothetical tag movements (large black arrows), were subset and the current averaged to estimate maximum flow rates at surface, mid and bottom depth levels. Circles show the maximum expected detection range (200 m). Small grey arrows indicate flow during tag detection time.

Tag detection data were compared against wind and visibility data sourced from the Wick weather station (UK MET Office Data) and moon phase. Quality checking resulted in false detections being eliminated from the dataset; these included detections where signals were logged with identity codes which did not correspond to any of the tags, possibly as a result of logger artefacts as well as false positive detections that corresponded to actively used tags but the time and location of the detections were not consistent with other detections of the same tag.

3. Results

3.1 Fish detection

Thirty-four fish were tagged on 23rd-24th April 2016 and 27 were subsequently detected at the River ALS (Table 1). The total period over which individuals were first detected was from 28th April to 21st May. Individuals were continuously present near the River ALS over periods ranging from 2-18 minutes. Two fish (IDs 1121 and 1122) were repeatedly detected over a

period of four days although they reached and left the River ALS area on different dates. The range of timings of first detections from the outer marine array was from 20:31 hr to 02:14 hr (UTC) indicating that the fish were not migrating during the main hours of daylight. Twenty-six of the 27 fish detected at the River ALS were subsequently detected in the marine array. One track was discarded (ID 1130) at this stage as a result of quality control issues associated with an unexplained error in the logged timestamp. For the others, the delay between the last detection at the River ALS and the first detection in the marine ALS array (ca. 8 km distance) varied from five hours to 35 days with a median value of 24 hours. 82% of first detections in the marine array were at night and the range of timings was 20:20 to 04:16 UTC (Figure 3). However, four of the tags were detected in daylight times; Tag 1153 was detected 43 minutes before sunset, Tag 1121 detected 1 minute prior to sunset, Tag 1150 detected 19 minutes prior to sunset and Tag 1129 detected 1 hour and 7 minutes prior to sunset. A Wald–Wolfowitz runs test performed on the number of detections at each marine ALS station indicated the results differed significantly from random ($h=1$, $p=0.009$). The binomial GLM model results indicated that probability of detection was most affected by distance from the array ($F(1,24512) = 30187$, $p<0.05$). Current magnitude and direction were significant, however, with a lower effect on probability of detection ($F(1,24512) = 152$, $p<0.05$ & $F(1,24512)=6$, $p<0.05$ respectively).

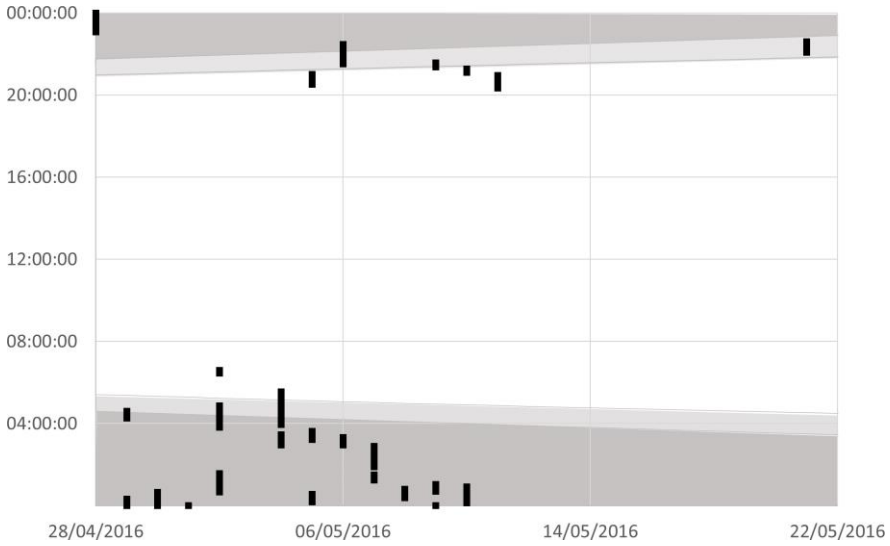

Figure 3: Timing of all marine detections with sunset, dusk and dawn times highlighted in grey.

3.2 Swimming depth

Swimming depth was repeatedly logged within in the marine array for three individuals. Swimming depth varied between 1 and 4 m. Water depth within the array varied between 7 and 30 m at lowest astronomical tide. Therefore, these smolts utilised the upper part of the water column during their time in the marine array with changes in bottom depth not affecting swim depth (Figure 4).

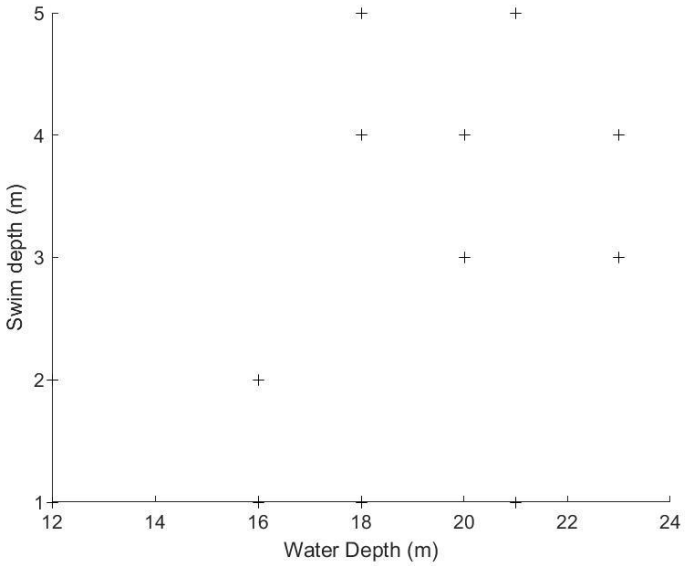

Figure 4: Swimming depths for three tagged fish in the marine ALS array against bottom depth of receiver stations.

227

228 3.3 Initial detections

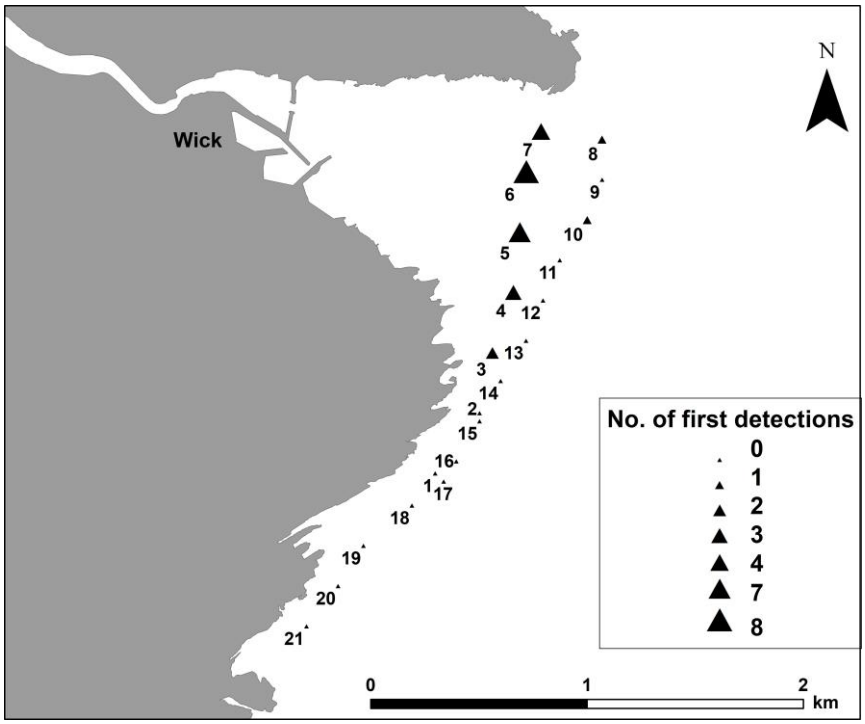

229

230 Figure 5 shows the number of occasions in which single transmitters were first logged at each
231 ALS position. As expected, all first detections occurred in the northern sector of the array by
232 North Headland, between ALS 3 and 7. As also expected, most (24 of 26) first detections
233 occurred in the inner component of the array and only two were logged in the outer component.
234 For occasions in which tags were detected simultaneously at multiple ALS, detection ranges
235 were estimated to be between 200 and 300 meters. Site range detection testing was completed
236 during array deployment showing detection ranges in excess of 200 m in calm conditions.

237

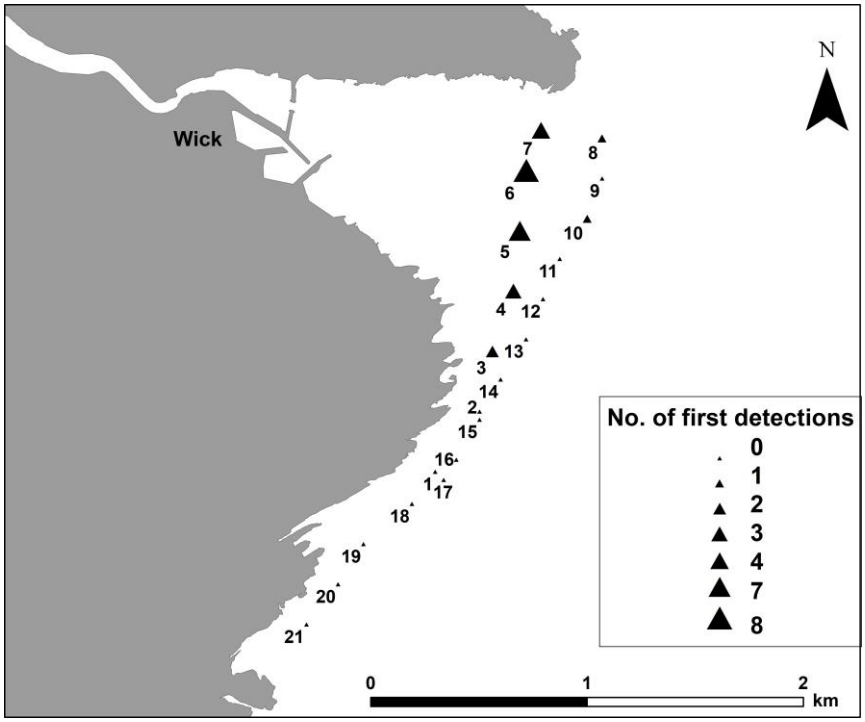

Figure 5: ALS locations for initial tag detections where station (triangles) size indicates number of detections, larger triangle for higher number of detections.

Tag detections were compared to other variables, tidal conditions, light conditions (including daylight and moonlight) and whether the tag detection pathway could be attributed to the tidal currents alone, through experimentation with free particle drift models (Table 1). The results showed only two tags were detected during times when the moon was above the horizon; Tag 1108: moon phase 60% illumination, 12° above horizon and Tag 1150: moon phase 16% illumination and 9° above horizon, limited moonlight. Two tags (1111 and 1130) were detected only once and were eliminated from further analysis as they were only represented by a single temporal data point. Tidal state showed that 18 tags were detected during or close to slack water conditions and 6 tags during flood or ebb tides, 16 tags were associated with ebb tide conditions whilst 8 tags were associated with flood tide conditions.

Table 1: Tag detection summary. The date, time, and duration of the first detection of each tag are shown. "Explained by model Flow only" denotes if the tag detection pathway is satisfactorily explained by modelled tidal current movements. Detections which included an additional vector of the fish swimming within the flow vector (Flow only = No) are highlighted in light grey. The mean model flow along the particle path is shown along with free particle calculated ground speed for path and time and distance for particle to complete path for tag detections. The night column denotes whether the tag detections occurred during daylight (no) or dark conditions (yes). Whether or not the moon was above the horizon at the time of the detections is included in brackets in the same column whereby; (m) moon above the horizon and visible.

Tag ID	First detection date	First detection time (UTC)	Detection duration (minutes)	Explained by model flow only	Model flow mean	Model free particle ground speed (m/s)	Mean particle ground direction	Tide state	Night	Free particle distance	Free particle time to reach time (mins)
101	08/05/2016	00:23	48	Yes	0.31	0.27013889	North	Ebb-Slack	Yes	778	48
102	21/05/2016	22:05	31	No	0.128	>0.128	South	Flood-slack	Yes	NaN	NaN
103	02/05/2018	00:53	342	Yes	0.14	0.04917617	East	Ebb-slack	Yes	776	263
1106	09/05/2016	00:00	62	Yes	0.28	0.27373737	North	Flood-slack	Yes	542	33
1107	06/05/2016	02:57	22	Yes	0.007	0.06363636	North	Ebb-slack	Yes	84	22
1108	29/04/2016	04:16	20	No	0.18	>0.018	South	Slack-ebb	Yes(m)	NaN	NaN
1109	28/04/2016	23:53	16	Yes	0.24	0.22291667	south	Slack-ebb	Yes	214	16
1110	28/04/2016	23:04	75	Yes	0.28	0.20895522	South	Flood -slack	Yes	840	67
1111	10/06/2016	04:09	n/a	Single Detection	NaN	NaN	NaN	Flood	Yes	NaN	NaN
1112	05/05/2016	0.0076389	22	Yes	0.18	0.16742424	North	Ebb	Yes	221	22
1119	07/05/2016	01:53	60	Yes	0.03	0.04482759	North	Ebb	Yes	156	58
1121	09/05/2016	21:22	12	Yes	0.3	0.24242424	East	Flood	No	160	11
1122	10/05/2016	00:08	47	Yes	0.18	0.09503546	East	Flood-slack	Yes	268	47
1123	06/05/2016	21:31	36	Yes	0.19	0.10075758	East	Flood-slack	Yes	133	22
1124	07/05/2016	01:15	15	Yes	0.35	0.34666667	North	Slack-Ebb	Yes	312	15
1125	30/04/2016	00:00	39	No	0.22	>0.22	South	Slack-flood	Yes	947	81
1126	29/04/2016	00:02	16	Yes	0.34	0.290625	South	flood	Yes	279	16
1127	06/05/2016	21:37	45	Yes	0.16	0.13809524	North	Flood-slack	Yes	290	35
1128	05/05/2016	03:13	24	Yes	0.04	0.03819444	South	Slack-flood	Yes	55	24
1129	11/05/2016	20:20	37	No	0.05	>0.05	North east	Slack-flood	No	NaN	NaN
1130	01/05/2016	00:00	n/a	Single detection	NaN	NaN	NaN	flood	Yes	NaN	NaN
1147	02/05/2016	03:49	63	Yes	0.18	0.15327381	South	flood	Yes	515	56
1148	06/05/2016	22:04	24	Yes	0.18	0.17222222	North	flood-slack	Yes	186	18
1150	10/05/2016	21:06	10	Yes	0.39	0.37037037	South	Slack-flood	No(m)	200	9
1151	02/05/2016	00:40	21	No	0.03	>0.05	North	Slack-flood	Yes	NaN	NaN
1152	04/05/2016	02:57	155	Yes	0.07	0.0625	South	Slack-flood	Yes	450	120
1153	05/05/2016	20:31	29	Yes	0.17	0.12666667	East	flood	No	38	5

3.4 Particle modelling

Although the model used in this study only used astronomical forcing, wind data from the Met Office MIDAS land surface observations shows no extreme high wind forcing events during the detection times. Modelling showed tag detection timings for the initial first pass through the marine array were consistent with tidal current patterns; however, after the tags left the marine array, they were not detected on subsequent tides. Tag 1147 (

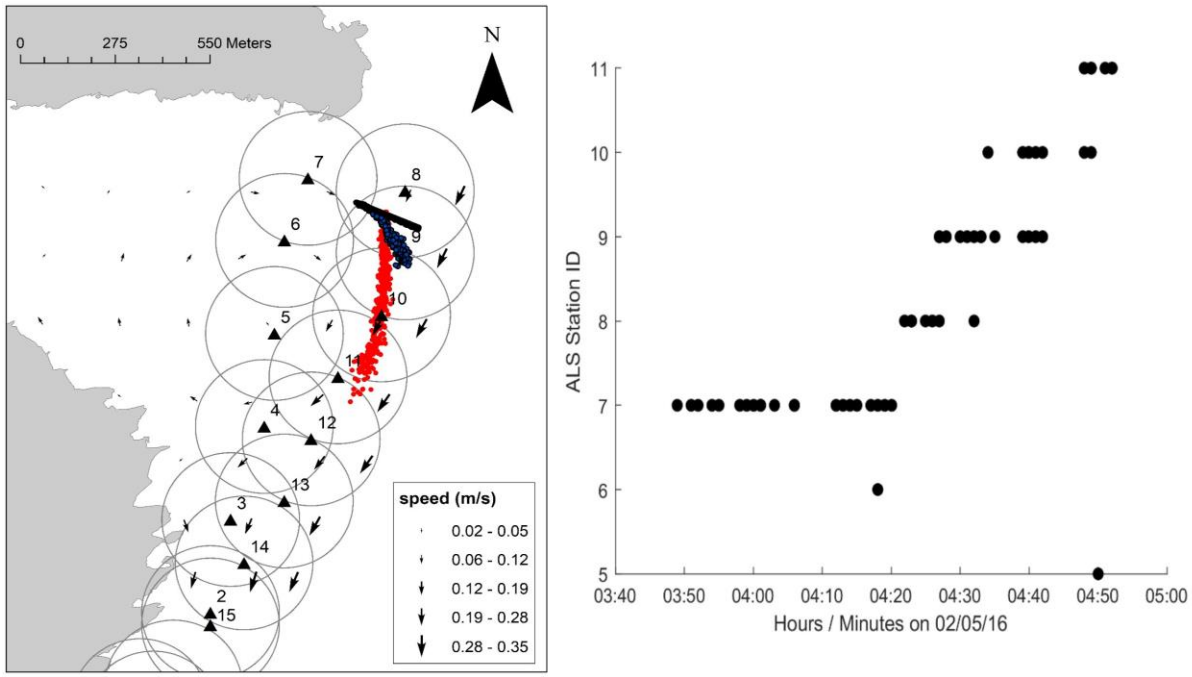

Figure 6) is an example of where a detection path could be explained by a free drifting particle. In all cases free drifting particles were released into the model on a line in approximate region of first detection and under the influence of the tidal currents until the last detection time.

Tag detection paths followed currents when tidal currents in the vicinity of the ALS exceeded approximately 0.2 m/s in all but two cases, based on an estimated 200-m detection radius of receivers. Tag 1107 and Tag 1128 movement paths were also explicable by the currents alone although the currents speeds were relatively low (0.1 and 0.09 m/s maximum current speed at times of detection within vicinity of free moving particles, Table 1). After initial tag detection,

for the tags explained by the current, 7 moved south, 7 moved north and 5 moved eastwards. Of the tags not explained by the current, 3 moved south and 2 moved northwards.

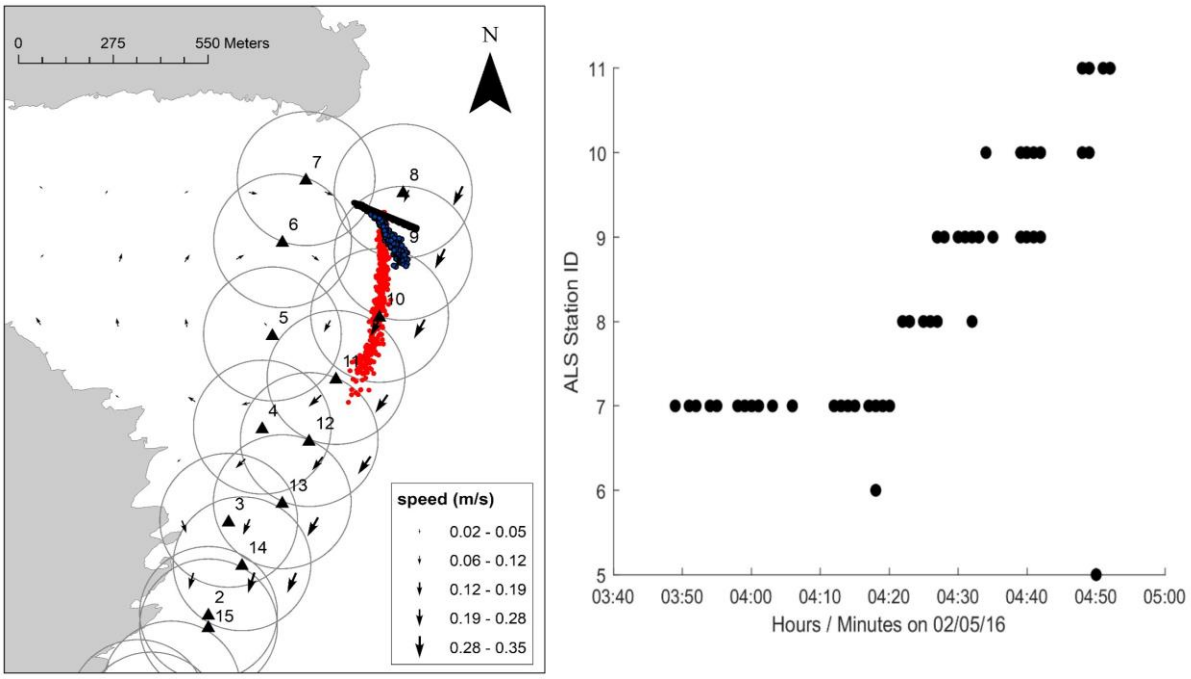

Figure 6: Tag 1147; (left) particle modelling showing the particle release location, Note particles released equally along line length (straight line), particle locations at half the run-time (blue dots) and final particle positions (red dots) the maximum ALS detection range (200 m, black circles) and the flow speed / direction, (right) tag detection timings at ALS stations for tag 1147.

3.5 Drift over subsequent tides

Particle modelling also showed free-drifting particles trapped by the tidal current would have been detectable in the marine array for several tides as the flowed through the marine array in subsequent ebb and flood tides; all of the fish detected in the marine array were detected only on one tide suggesting that they left the area rapidly after passing through the array immediately after leaving the river. Particle-drift simulations were run over several tidal cycles beyond the last detection of each tag to estimate what paths particles may take by astronomical tidal action alone. The example in Figure 7 is a 48-hour simulation for Tag 1125. One of the 500 particles injected into the model is highlighted as an example. The particle highlighted is on the extreme east of the particle injection line at a position where tidal currents have the highest influence. The point shows multiple interactions with the marine array (dark grey area, Figure 7) over the

period of 48 hours, all other simulated particles had similar multiple interactions with the marine array. A similar pattern occurred for all other simulations where particles had multiple interactions with the marine array over several tidal cycles. Simulations showed few particles eventually escaping to the north, whilst the majority became trapped for longer periods in near coastal tidal currents and bay eddies.

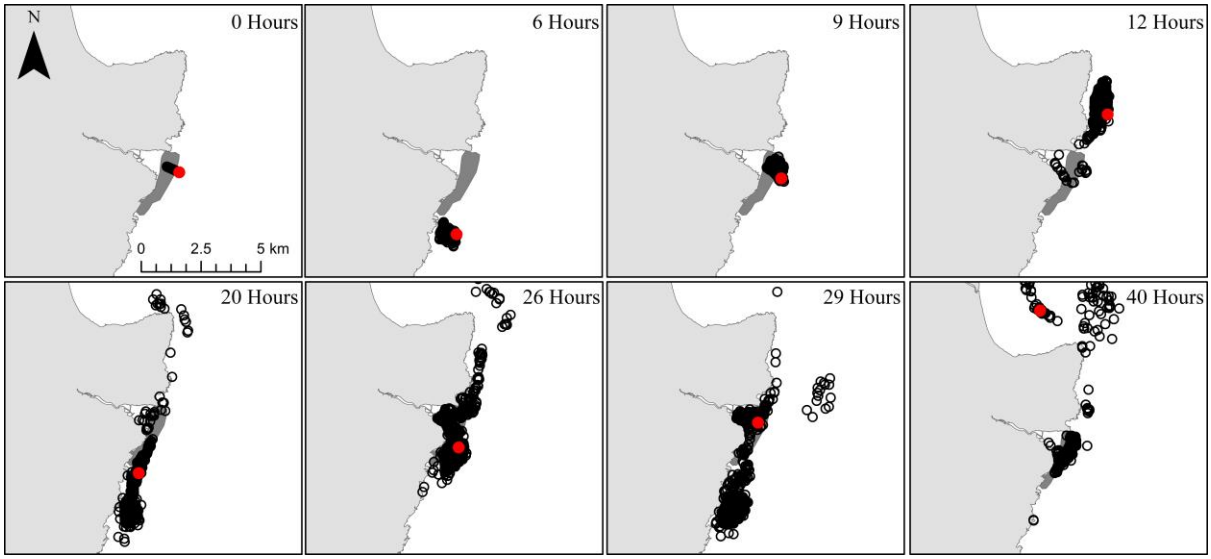

Figure 7: 48-hour simulation of 500 particles released perpendicular to current in estimated position of first detection of Tag 1125. Dark grey zone indicates 200 m buffer around marine array vicinity. Example point, single drifting particle (red) shows multiple interactions with tidal array assuming 200-m detection range.

3.6 Anomalies

Five of the 27 detection tracks were not explicable by tidal current movements from model results (Table 1, Tag IDs 102, 1108, 1125, 1129 and 1151). Of these 5 tags, 4 occurred in low-flow velocities (<0.2 m/s), these 4 tags moved in different directions to the mean current flow suggested by modelling results. The 5th tag which could not be explained by currents alone was associated with currents from 0.22-0.27 m/s (Tag 1125); however, the direction of travel was with the tidal flow. This tag also exhibited the fastest rate of movement at up to 0.48 m/s (1.72 km/hr) estimated by initial detection time to final detection time.

4. Discussion

This study used a 3-dimensional hydrodynamic model to improve understanding of how an array of receivers detects the movement of tagged fish. The model proved an important tool in understanding smolt behaviour from tag movements in relation to hydrodynamics of the bay. The model agreed with the majority of tag movements (77.7%). Of the tracks which are explained by tidal currents, the model indicated these experienced current speeds in excess of 0.2 m/s.

After last detection at the River ALS, smolts rapidly migrated to the marine environment as indicated in previous studies (Halfyard et al. 2012; Lothian et al. 2016; Nicola et al. 2018). Marine detection mostly occurred after sunset and prior to sunrise. Four exceptions were first registered close to sunset. These findings are in line with other published results (Thostad et al. 2016; Lothian et al. 2017). Haraldstad et al. (2016) found most river and marine migration success linked to night, potentially due to predator avoidance.

Three of the smolts were monitored for depth. This showed they stayed near the surface whilst detected in the outer marine array. This agrees with other studies finding that after initial marine migration, smolt stay near the surface (Thorstad et al. 2012). Estimated tag movement speeds show faster than maximum suggested smolt swim speed, 0.25 m/s (0.9 km/hr) but comparable with other studies where smolt utilize currents (Thorstad et al. 2012; Lothian et al. 2017; Newton et al. 2017).

Two hypotheses have been suggested previously of migratory behaviour in juvenile Atlantic salmon in the marine environment, either they rely heavily on passive transport, or they have directional component to their migration (Ounsley et al. 2020). All tags which were detected by the marine array are only detected on the same tidal phase as the initial detection and are not detected in subsequent tidal phases. Passive particle modelling suggests particles would

interact with the marine array several times over subsequent tidal cycles, becoming trapped in the ebb and flood currents which flow approximately north to south. On the contrary, the tags were not detected in the marine array in subsequent tidal phases, suggesting either the smolt were actively altering their vector by swimming, or they were prevented returning to the array (predation).

These results point to transitional behaviour of the smolt. A first stage of river migration behaviour is defined by active swimming during a narrow time window to enter the marine environment. Once in the marine environment, during an initial marine behaviour stage, the smolt may remove themselves from the influence of coastal waters. This raises questions as to whether there are further behaviour changes occurring proceeding this. No strong evidence of a preferred north or south trajectory was found with 66% of the tags were associated with ebb tide whilst 34% were associated with flood tide conditions. However, this may be a subsequent behaviour at a later point in migration, possibly changing direction after leaving the influence of near-shore coastal waters for migratory routes leading to feeding grounds in the Northeast Atlantic (Ounsley et al. 2020). It is not known whether smolt will continue to avoid near-shore conditions or use them intermittently, such as returning to stronger currents when direction is favourable, for example using only ebb currents and returning to deeper water for the flowing flood tide with a net north movement, or if tidal channels with extreme conditions like the Pentland Firth are utilised or avoided. If they salmon continue to utilise currents during their migration it may bring them into direct contact with renewable energy developments. Renewable energy developments are increasing worldwide with a 13% increase in growth in 2019 (Chowdhury et al. 2020). There are several developments planned and at early stages around Scottish waters including the Pentland Frith and Orkney waters, where strong tidal currents are present. Travel through these areas would provide a low-energy path for smolt to

reach richer feeding grounds. In addition, in deeper waters with low flow, offshore wind energy developments exist, with smolts potentially interacting with high voltage subsea cables.

Subsequent tagging and modelling work are required to investigate smolts' movements after leaving the area of their initial marine migration. Smolt interactions with marine renewable developments are poorly understood due to poor understanding of how and where the smolt move during their migration. This study was an attempt to track the first stage of this journey. The results will be used to inform initialisation of further tagging efforts and marine listening station array design to track the route of smolts as they migrate along the Scottish coastline, together with high-resolution particle drift models using particles which mimic fish behaviour, for example with traits of preferred swimming direction, swimming depth, and starting position (nearest point offshore removed from near-shore current influence) and with current utilisations preferences.

In future, it may prove possible to extrapolate from modelling studies to guide sequential studies of the dispersal of migrants, focussing necessarily limited technical resources for tracking on the predicted pathways of fish moving through very large areas of sea. In order to achieve this, adequate hydrodynamic models and realistic biological inputs for the point and timing of entry of fish to the model domain and their subsequent behaviour in the domain will be needed at each stage.

5. Acknowledgements

The involvement of the community through the FCRT demonstrated high levels of local interest extending to practical advice and material support from both commercial and sports fishermen. Beatrice Offshore Windfarm Ltd. Community Fund contributed to the receiver deployments.

6. References

Aldvén, D, Degerman, E. & Höjesjö, J. 2015. Environmental cues and downstream migration of anadromous brown trout (Salmo trutta) and Atlantic salmon (Salmo salar) smolts. Boreal Environment Research. 20: 35–44

Alerstam T, Hedenstrom A & Akesson S. 2003. Long- distance migration: Evolution and determinants. Oikos, 103, 247–260

Gill, A., Bartlett, M., & Thomsen, F. 2012. Potential interactions between diadromous fishes of UK conservation importance and the electromagnetic fields and subsea noise from marine renewable energy developments. Journal of Fish Biology, 81, 664–695.

Buck, R. & Youngson, A. 2006. The downstream migration of precociously mature Atlantic salmon, Salmo salar L, parr in autumn; its relation to the spawning migration of mature adult fish. Journal of Fish Biology. 20. 279 - 288. 10.1111/j.1095-8649.1982.tb04709.x.

Byron C. J., Pershing, A. J., Stockwell J. D., Huijie X. & Kocik J. 2014. Migration model of post-smolt Atlantic salmon (Salmo salar) in the Gulf of Maine. Fisheries Oceanography. 23. 10.1111/fog.12052.

Chaput G., Carr J., Daniels J., Tinker S., Jonsen I., Whoriskey F., & Durif C. 2018. Atlantic salmon (Salmo salar) smolt and early post-smolt migration and survival inferred from multi-year and multi-stock acoustic telemetry studies in the Gulf of St. Lawrence, northwest Atlantic, ICES Journal of Marine Science, https://doi.org/10.1093/icesjms/fsy156

Chowdhury, M.S., Rahman, K.S., Selvanathan, V. et al. 2020. Current trends and prospects of tidal energy technology. Environ Dev Sustain (2020). https://doi.org/10.1007/s10668-020-01013-4

Clements, S., Jepsen, D., Karnowski, M. and Schreck, C.B. 2005, Optimization of an Acoustic Telemetry Array for Detecting Transmitter-Implanted Fish. North American Journal of Fisheries Management, 25: 429-436. https://doi.org/10.1577/M03-224.1

Dadswell, M. J., Spares, A. D., Reader, J. M. & Stokesbury, M.J.W. 2010. The North Atlantic subpolar gyre and the marine migration of Atlantic salmon Salmo salar: the 'Merry-Go-Round' hypothesis. Journal of Fish Biology, 77: 435-467. doi:10.1111/j.1095-8649.2010.02673.x

Davies, M. 2006. Psed4.3 A Lagrangian Sediment Transport Model Technical Documentation. Canada: Pacific International Engineering Corp.

Dieperink, C., Bak, B. D., Pedersen, L. F., Pedersen, M. I., and Pedersen, S. 2002. Predation on Atlantic salmon and sea trout during their first days as postsmolts. Journal of Fish Biology, 61: 848–852.

Dolotov S. I. 2006. The effects of water temperature on the migration of smolts of the Atlantic salmon Salmo salar L. J. Ichthyol. 46 (Suppl. 2): S194. https://doi.org/10.1134/S0032945206110099

Egbert G. D, & Erofeeva S. Y. 2002. Efficient inverse modelling of Barotropic Ocean tides. Journal of Atmospheric and Oceanic Technology 19.2: 183-204.

Friedland K. D. 1998. Ocean climate influences on critical Atlantic salmon (Salmo salar) life history events. Canadian Journal of Fisheries and Aquatic Sciences, 55 (Suppl.) 119–130.

Galland J. C., Goutal N., Hervouet J. M. 1991. TELEMAC: A New Numerical Model for Solving Shallow Water Equations. Advances in Water Resources 14(3), 138–148. doi:10.1016/0309-1708(91)90006-A

Godfrey, J. D., Stewart, D. C., Middlemas, S. J., & Armstrong, J. D. 2015. Depth use and migratory behaviour of homing Atlantic salmon (Salmo salar) in Scottish coastal waters, ICES

Journal of Marine Science, Volume 72, Issue 2, Pages 568–575, https://doi.org/10.1093/icesjms/fsu118

Nicola G. G., Elvira B., Jonsson B., Ayllón D., Almodóvar A. 2018. Local and global climatic drivers of Atlantic salmon decline in southern Europe. Fish Res 198: 78–85.

Halfyard E. A., Gibson A. J., Ruzzante D. E., Stokesbury M. J. & Whoriskey F. G. 2012. Estuarine survival and migratory behaviour of Atlantic salmon Salmo salar smolts. Journal of Fish Biology, 81: 1626-1645. doi:10.1111/j.1095-8649.2012.03419.x

Haugland, M., Holst, J. C., Holm, M. & Hansen, L. P. 2006. Feeding of Atlantic salmon (Salmo salar L.) post-smolts in the Northeast Atlantic, ICES Journal of Marine Science, Volume 63, Issue 8, Pages 1488–1500, https://doi.org/10.1016/j.icesjms.2006.06.004

Haraldstad T., Kroglund F., Kristensen H., Jonsson B. & Haugen T. O. 2016 Diel migration pattern of Atlantic salmon (Salmo salar) and sea trout (Salmo trutta) smolts: an assessment of environmental cues. Ecology of Freshwater Biology.

Harding H., Bruintjes R., Radford A. N. & Simpson S. D. 2016. Measurement of Hearing in the Atlantic salmon (Salmo salar) using Auditory Evoked Potentials, and effects of Pile Driving Playback on salmon Behaviour and Physiology. Marine Scotland Science; Scottish Marine and Freshwater Science Vol 7 No 11

Hedger, R. D., Martin, F., Dodson, J, J., Hatin, D., Caron, F., and Whoriskey, F. G. 2008. The optimized interpolation of fish positions and speeds in an array of fixed acoustic receivers. – ICES Journal of Marine Science, 65: 1248–1259.

Holst J. C., Shelton R., Holm M., Hansen L. P. 2000. Distribution and possible migration routes of post-smolt Atlantic salmon in the North-east Atlantic. In The Ocean Life of Atlantic Salmon:

452 Environmental and Biological Factors Influencing Survival, pp. 65–74. Ed. by D. Mills.
453 Fishing New Books, Oxford.

454 Jensen A. J., Finstad B., Fiske P., Hvidsten N. A., Rikardsen A. H. & Saksgård L. 2012 Timing
455 of smolt migration in sympatric populations of Atlantic Salmon (Salmo Salar), Brown trout
456 (Salmo Trutta), and Arctic Char (Salvelinus Alpinus). Canadian Journal of Fisheries and
457 Aquatic Sciences, 2012, 69:711-723,https://doi.org/10.1139/f2012-005

458 Johansson, D., Laursen, F., Fernö, A., Fosseidengen, J. E., Klebert, P., Stien, L. H., Oppedal,
459 F. 2014. The interaction between water currents and salmon swimming behaviour in sea
460 cages. PloS one, 9(5), e97635. doi:10.1371/journal.pone.0097635

461 Kuparinen A, O'Hara R. B. & Merila J. 2009. Lunar periodicity and the timing of river entry
462 in Atlantic salmon Salmo salar L. Journal of Fish Biology 74, 2401–2408 doi:10.1111/j.1095-
463 8649.2009.02255.

464 Lothian A. J, Newton M., Barry J., Walters M., Miller R. C. & Adams C. E. 2017. Migration
465 pathways, speed and mortality of Atlantic Salmon (Salmo salar) smolts in a Scottish river and
466 the near-shore coastal marine environment. Ecol. Freshwater Fish. 2017;00:1–10.
467 https://doi.org/10.1111/eff.12369

468 Lefèvre, M. A., Stokesbury, M. J. W., Whoriskey, F. G. & Dadswell, M. J., 2012. Atlantic
469 salmon post-smolt migration routes in the Gulf of St. Lawrence, ICES Journal of Marine
470 Science, Volume 69, Issue 6, July 2012, Pages 981-990, https://doi.org/10.1093/icesjms/fss092

471 Malcolm, I. A., Godfrey, J. & Youngson, A. F. 2010. Review of migratory routes and behaviour
472 of atlantic salmon, sea trout and european eel in scotland's coastal environment: implications
473 for the development of marine renewables. Scottish Marine and Freshwater Science Volume 1
474 No 14

475 Malcolm, I., Millar, C. & Millidine, K. 2015. Spatio-temporal variability in Scottish smolt
476 emigration times and sizes. Scottish Marine and Freshwater Science Vol 6 No 2, Affiliation:
477 Marine Scotland Science. 10.7489/1590-1.

478 McCormick S. D., Hansen L. P., Quinn T. P. & Saunders R. L. 1998. Movement, migration,
479 and smolting of Atlantic salmon (Salmo salar). Canadian Journal of Fisheries and Aquatic
480 Sciences 55, 77–92.

481 Moriarty, P. E., Byron, C. J., Pershing, A. J. 2016. Predicting migratory paths of post-smolt
482 Atlantic salmon (Salmo salar). Mar Biol 163, 74. https://doi.org/10.1007/s00227-016-2847-5

483 Mork K. A., Gilbey J.., Hansen L. P., Jensen A. J., Jacobsen J. A., Holm M., Holst J. C.,
484 Maoileidigh N. O., Vikebo F., McGinnity P., Melle W., Thomas K., Verspoor E. & Wennevik
485 V. 2012. Modelling the migration of post-smolt Atlantic salmon (Salmo salar) in the Northeast
486 Atlantic. ICES Journal of Marine Science, vol 69, no. 9, pp. 1616-1624.
487 DOI: 10.1093/icesjms/fss108

488 Newton M, Main R. & Adams C. 2017. Atlantic Salmon Salmo Salar smolt movements in the
489 Cromarty and Moray Firths, Scotland. Beatrice Offshore Windfarm report LF000005-REP-
490 1854

491 Newton, M., Barry, J., Dodd, J. A., Lucas, M.C., Boylan, P. & Adams, C.E. 2016. Does size
492 matter? A test of size-specific mortality in Atlantic salmon Salmo salar smolts tagged with
493 acoustic transmitters. Journal of Fish Biology 89(3): 1641-1650.

494 Nicola G. G., Elvira B., Jonsson B., Ayllón D. & Almodóvar A. 2018. Local and global climatic
495 drivers of Atlantic salmon decline in southern Europe, Fisheries Research, Volume 198, Pages
496 78-85, ISSN 0165-7836, https://doi.org/10.1016/j.fishres.2017.10.012.

497 Niezgoda, G., Benfield, M., Sisak, M., Anson, P., 2002. Tracking acoustic transmitters by code
498 division multiple access (CDMA)-based telemetry. In: Thorstad, E.B., Fleming, I.A., Næsje,
499 T.F. (Eds.), Aquatic Telemetry: Proceedings of the Fourth Conference on Fish Telemetry in
500 Europe vol. 165. Springer, Netherlands, pp. 275–286

501 Økland F., Thorstad E. B., Finstad B., Sivertsgard R., Plantalech N., Jepsen N. & Mckinley R.
502 S. 2006. Swimming speeds and orientation of wild Atlantic salmon post-smolts during the first
503 stage of the marine migration. Fisheries Management and Ecology 13. 271-274.
504 10.1111/j.1365-2400.2006.00498.x.

505 Ounsley, J. P., Gallego, A., Morris, D. J. & Armstrong, J. D. 2020. Regional variation in
506 directed swimming by Atlantic salmon smolts leaving Scottish waters for their oceanic feeding
507 grounds—a modelling study, ICES Journal of Marine Science, Volume 77, Issue 1, January-
508 February 2020, Pages 315–325, https://doi.org/10.1093/icesjms/fsz160

509 Popper AN, Hawkins, A; Eds. 2012. The effect of noise on aquatic life. Springer

510 Quinn T. P. 1980. Evidence for celestial and magnetic compass orientation in lake migrating
511 sockeye salmon fry, Journal of comparative physiology. 137, 3, 234-248.

512 Rahman, A. A. & Venugopal, V. 2015. Inter-Comparison of 3D Tidal Flow Models Applied
513 to Orkney Islands and Pentland Firth. Conference: 11th European Wave and Tidal Energy
514 Conference (EWTEC 2015) Nantes, France

515 Riley W. D., Eagle M. O., & Ives J. 2002. The onset of downstream movement of juvenile
516 Atlantic Salmon, Salmo salar L. in a chalk stream. Fisheries Management and Ecology, 9, 87-
517 94

518 Russell, I. C., Aprahamian, M. W., Barry, J., Davidson, I. C., Fiske, P., Ibbotson, A. T.,
519 Kennedy, R. J., Maclean, J. C., Moore, A., Otero, J., Potter, E. C. E., and Todd, C. D. 2012.

520 The influence of the freshwater environment and the biological characteristics of Atlantic
521 salmon smolts on their subsequent marine survival. – ICES Journal of Marine Science, 69:
522 1563–1573.

523 Sanderson B., Buhariwalla C., Adams M., Broome J., Stokesbury M. & Redden A. 2016.
524 Quantifying Detection Range of Acoustic Tags for Probability of Fish Encountering MHK
525 Devices. Renewable Energy 97:746-756

526 Scruton D. A., McKinley R. S., Booth R. K., Peake S. J. & Goosney R. F. 1998. Evaluation of
527 swimming capability and potential velocity barrier problems for fish Part A. Swimming
528 performance of selected warm and cold-water fish species relative to fish passage and fishway
529 design. CEA Project 9236 G 1014, Montréal, Québec.

530 Singh, L Downey, N. J., Roberts, M. J., Webber, D. M., Smale, M. J., van den Berg, M. A.,
531 Harding, R. T., Engelbrecht D. C. & Blows B. M. 2009. Design and calibration of an acoustic
532 telemetry system subject to upwelling events, African Journal of Marine Science, 31:3, 355-
533 364, DOI: 10.2989/AJMS.2009.31.3.8.996

534 Strøm, J. F., Thorstad, E. B., Hedger, R. D. 2018. Revealing the full ocean migration of
535 individual Atlantic salmon. Animal Biotelemetry 6, 2. https://doi.org/10.1186/s40317-018-
536 0146-2

537 Tang J. & Wardle C. S. 1992. Power output of two sizes of Atlantic Salmon (Salmo Salar) at
538 their maximum sustained swimming speeds. Journal of Experimental Biology 166: 33-46;

539 Thorstad E. B., Whoriskey F., Uglem I., Moore A., Rikardsen A. H. & Finstad B. 2012. A
540 critical life stage of the Atlantic salmon Salmo salar: behaviour and survival during the smolt
541 and initial post-smolt migration. J. Fish. Biol. 2012 Jul; 81(2):500-42. doi: 10.1111/j.1095-
542 8649.2012.03370.x.

543 UK Meteorological Office. MIDAS Land Surface Stations data (1853-current), [Internet].
544 British Atmospheric Data Centre, 2006, Date of citation. Available from
545 http://badc.nerc.ac.uk/data/ukmo-midas

546 WWF 2001. The Status of Wild Atlantic Salmon: A River by River Assessment. Washington,
547 DC, USA: WWF-US.

548

549 Additional data sources:

550

551 Tides for fishing: https://tides4fishing.com/uk/scotland/wick; Accessed 14/02/19

552 Moon Locator: https://futureboy.us/fsp/moon.fsp; Accessed 14/02/19